# Field observation of fluid circulation patterns in a normal fault system

Jerry P. Fairley and Jennifer J. Hinds

Department of Geological Sciences, University of Idaho, Moscow, Idaho, USA

Received 22 June 2004; revised 24 August 2004; accepted 10 September 2004; published 9 October 2004.

[1] Faults are often assumed to be either barriers or conduits for subsurface fluid flow, although they may act as both, depending on the hydraulic architecture of the fault and the direction of flow with respect to the fault plane. Here we use high-resolution (5 × 5 m spacing) ground temperature measurements to track geothermal discharge in the step-over region of an active échelon normal fault in southeast Oregon. Our analysis demonstrates that the fault acts as a combination conduit-barrier system and reveals complex, 3-dimensional circulation patterns in the area of the fault step-over. Although complex flow circulation patterns are likely to be present in most fault-controlled flow systems, they are generally neglected in conceptual and numerical models. Improved understanding of this aspect of subsurface fluid flow is essential for developing better models of fault hydrology. *INDEX TERMS:* 1829 Hydrology: Groundwater hydrology; 5104 Physical Properties of Rocks: Fracture and flow; 8010 Structural Geology: Fractures and faults; 8045 Structural Geology: Role of fluids; 8135 Tectonophysics: Hydrothermal systems (8424). **Citation:** Fairley, J. P., and J. J. Hinds (2004), Field observation of fluid circulation patterns in a normal fault system, *Geophys. Res. Lett.*, *31*, L19502, doi:10.1029/2004GL020812.

## 1. Introduction

[2] Faults have been shown to act as barriers to subsurface fluid flow [*Antonellini and Aydin*, 1994; *Mayo et al.*, 2003], conduits [*Barton et al.*, 1995; *Curewitz and Karson*, 1997; *Fairley et al.*, 2003], or a combination of barrier and conduit [*Smith et al.*, 1990; *Caine et al.*, 1996; *Evans et al.*, 1997; *Jourde et al.*, 2002], depending on the amount of fracturing and cataclasis, the extent of alteration and precipitation, composition of the protolith, and the direction of flow with respect to the fault plane. Furthermore, faults have been shown to be highly heterogeneous [*Jourde et al.*, 2002; *Fairley et al.*, 2003; *Fairley and Hinds*, 2004; *Kato et al.*, 2004], and their properties may change over time [*Smith et al.*, 1990; *Caine et al.*, 1996; *Curewitz and Karson*, 1997; *Evans et al.*, 1997].

[3] The spatially and temporally complex nature of faults makes their impact on fluid flow difficult to evaluate. Ideally, fluid circulation patterns could be observed in situ in an active fault zone, and areas that act locally within the fault as conduits or barriers to flow could be uniquely identified. This type of observation is generally not possible in active systems; as a result, fluid circulation patterns are usually inferred from geochemical evidence [*Martin et al.*, 2000; *Favara et al.*, 2001; *Mayo et al.*, 2003], borehole measurements [e.g., *Barton et al.*, 1995], or observations of paleofluid migration paths in exhumed, inactive fault zones [*Caine et al.*, 1996; *Jourde et al.*, 2002]. Here we use ground temperature measurements to obtain a high-resolution image of fluid circulation in the step-over region of a left stepping échelon normal fault. The data permit direct identification of the roles played by the various components of the fault in controlling fluid migration patterns, and are of sufficient resolution to allow estimation of the architectural indices of *Caine et al.* [1996].


0094-8276/04/2004GL020812$05.00

## 2. Site Description

[4] The study area is located on a north-northeast striking normal fault north of Borax Lake, in the Alvord Basin of southeast Oregon (Figure 1). The Alvord Basin is a north-south trending graben, typical of the northern Great Basin extensional province. The basin is bounded to the west by Steens Mountain and the Pueblo Mountains, and to the east by the Trout Creek Mountains. Faults in the Alvord Basin generally strike northeast to southwest, and cut sequences of Miocene-age volcanics, including basalts, andesites, and tuffs. Bedrock within the Alvord Basin is largely overlain by thick deposits of poorly lithified alluvium and playa lake sediments; however, geophysical evidence indicates that the Borax Lake fault bounds a buried horst that extends to within a few meters of the land surface the vicinity of the geothermal springs [*Blackwell et al.*, 1986]. Topographic relief across the fault is up to 3 m in some areas, which drives shallow discharge in a predominantly easterly direction, away from the fault. The overall flow of groundwater in the basin is northward towards Alvord Lake, but this regional gradient does not appear to exert significant influence over shallow lateral flow in the study area.

[5] Approximately 175 geothermal springs outline the trace of the left-stepping fault that extends 1 km north from Borax Lake (Figure 1). Commercial evaluation of the Borax Lake geothermal resource was halted to protect an endangered species of chub that inhabits Borax Lake [*Schneider and McFarland*, 1995], but geochemical investigations indicate the thermal springs are probably nonmagmatic, and originate from a reservoir temperature of approximately 200 to 250°C [*Cummings et al.*, 1993; *Koski and Wood*, 2004].

## 3. Data Collection and Analysis

[6] The present study focuses on a 100 × 100 m area in the step-over region of the Borax Lake fault (Figure 1). Ground temperatures were measured on a 5 × 5 m grid spacing using handheld digital thermometers and heavy-duty thermocouple probes 0.2 m in length. Lithified materials in the area of the step-over are obscured by a thin (0 to ~5 m) covering of precipitates, travertine, and poorly developed

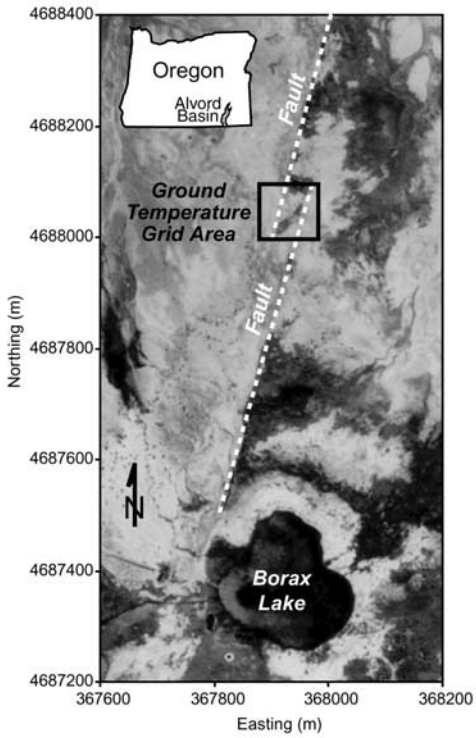


**Figure 1.** The location of the study area in the Alvord Basin of southeast Oregon. The study was conducted in a 100 × 100 m area encompassing the step-over region of the Borax Lake fault. Vegetation in the fault step-over (visible as darker areas) is bounded by the two fault splays, reflecting structural controls on shallow groundwater flow (air photo by USGS).

soil. Because the water table is near or at the land surface, the measured temperatures are assumed to be representative of the shallow subsurface fluids. All data were taken during one day in May 2004, to minimize the influence of diurnal temperature fluctuations.

[7] The measured ground temperatures range from a low of 12°C to a high of 52°C near one of the geothermal springs included within the study area. A contour plot of temperatures in the step-over region of the Borax Lake fault is shown in Figure 2, along with three temperature profiles oriented perpendicular to the strike of the fault.

## 4. Discussion and Conclusions

[8] A number of investigators have used subsurface temperatures to infer aquifer properties [*Bredehoeft and Papadopulos*, 1965; *Lu and Ge*, 1996; *Ge*, 1998], and a combination of temperature measurements and geochemical data was recently applied to delineate horizontal fluid flow paths [*Carreón-Diazconti et al.*, 2003]. Temperature data is usually not available at an adequate resolution to allow imaging of subsurface phenomena without supporting data (e.g., geochemical sampling); however, for the small area of our study it was possible to achieve a sufficient density of measurements to detect fluid migration in the shallow subsurface, and thus infer the influence of the fault splays on groundwater flow paths.

[9] The data in Figure 2 show elevated temperatures along the east-side damage zones of the two fault splays. Transport of heat in the Borax Lake fault is dominated by fluid convection [*Fairley and Hinds*, 2004]; therefore, these higher-temperature areas correspond to zones of geothermal fluid flow moving vertically, parallel to the plane of the fault. The highest temperatures generally coincide with the locations of geothermal springs, which represent the highest-permeability flow paths through the damage zone, but locally high temperatures indicate fluid upwelling through the damage zones in areas not necessarily correlated with visible springs. For example, spring B1110 (see Figure 2) is the northernmost spring on the eastern splay, and the only spring on the east splay included within the study area, but elevated temperatures indicate geothermal fluid is discharging from much of the east-side damage zone of the eastern fault splay.

[10] Examination of the vegetation patterns in the aerial photo of Figure 1 imply that discharge from the Borax Lake fault is generally moving eastward, away from the fault, and this appears to be supported by the temperature data

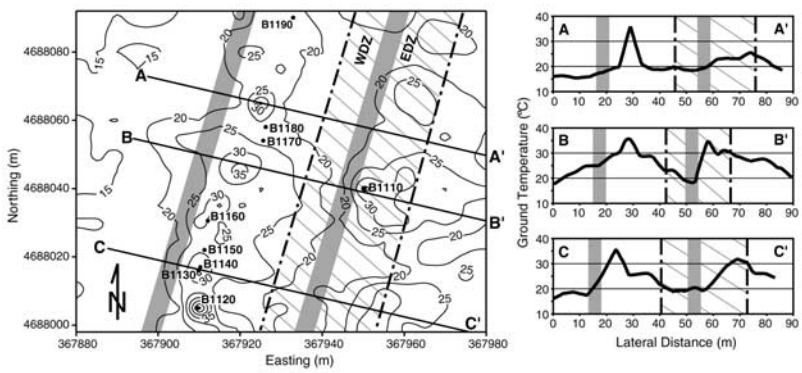


**Figure 2.** Temperature distributions in the Borax Lake fault step-over region. Left: Contour plot of temperatures measured on a 5 × 5 m grid spacing over the study area. Geothermal springs are labeled with spring survey "B" numbers. Approximate locations of fault cores are marked with grey bands, while the approximate extent of east and west side damage zones associated with the east fault splay are delineated with dashed lines and labeled "EDZ" and "WDZ," respectively. Right: Temperature plots for the three profiles marked on the contour plot, orientated approximately normal to the fault strike. The grey bands indicate the locations of the inferred low-permeability fault cores, while the dashed lines delineate the damage zones of the east fault splay.

associated with the east fault splay. The 20 and 25°C contour lines and, to a lesser extent, the 30°C contour are closely spaced near the core of the east splay, and more widely spaced away from the core, consistent with discharge from the damage zone cooling and moving laterally away from the fault to the east. The resulting asymmetric temperature distribution is most evident between 50 and 90 m in profile B–B′ (Figure 2), and somewhat less clearly in profile C–C′. Profile A–A′ shows only a broad, low temperature peak between 60 and 90 m as the eastern splay pinches out, and thermal discharge from the splay declines in the northeastern part of the study area.

[11] Temperatures near the western splay of the fault show a different pattern than those associated with the east splay. All three temperature profiles are more symmetric and have higher peak temperatures over the inferred damage zone, generally located between 20 and 35 m, as compared to the peaks between 50 and 90 m, attesting to the higher permeability and greater quantity of thermal discharge associated with this damage zone. Furthermore, temperatures at the western margin are the lowest in the study area, averaging about 5°C cooler than the next warmest areas, which implies a low-permeability fault core associated with the western fault splay is blocking discharge from migrating westward. Discharge from the western fault splay also appears to be blocked by the low-permeability core of the neighboring splay, and may be diverted northwards along the trend of the fault, or downwards through the damage zone flanking the western side of the eastern splay (Figure 3). Although the temperature data in the contour plot of Figure 2 tend to favor this latter hypothesis, the distribution of vegetation visible in aerial photographs implies some northward migration of groundwater (Figure 1); this effect may be seasonal, or may represent a combination of horizontal flow to the north and vertical, downward flow into the damage zone of the eastern fault splay.

[12] On the basis of the preceding interpretations of the temperature data, we estimated the extent of core and damage zones associated with the eastern fault splay. Our estimates of the core width vary from a maximum of 10 m to a minimum of about 4 m, while our estimates for the east and west side damage zones bounding the eastern splay are 16–10 m and 13–7 m (maximum-minimum), respectively. The ratio of the width of the fault zone to its length (approximately 1 km [*Fairley et al.*, 2003]) is consistent with the scaling relationship proposed by *Vermilye and Scholz* [1998], who found the width of the process zone (combined fault core and damage zones) to scale with fault trace length as $P/L \sim 10^{-2}$ for faults in the Shawangunk Mountains of New York. Furthermore, although our data do not allow precise measurement of the core and damage zone widths, estimates of the ratio of the width of the damage zones to the total fault width fall within a relatively narrow range between 0.63 and 0.81. The ratio of damage zone width to total fault width (measured normal to the fault plane) was used by *Caine et al.* [1996] as a means of classifying fault hydraulic architecture: values near zero indicate faults with well-developed cores that act as barriers to flow, while faults with values near one possess extensive damage zones, poorly developed cores, and generally exhibit conduit-like behavior. *Caine et al.* [1996] found a mean ratio of 0.79 and a range of 0.33 for Fault 6 at Traill Ø, East Greenland, which they described as a "conduit-barrier fluid flow system" with "relatively uniform architecture." The investigators noted of the Traill Ø fault that "...silicified breccia and clay-rich gouge in the core would act as barriers to flow normal to the fault zone, and open fractures in the damage zone would act as a conduit for flow parallel to the fault zone" [*Caine et al.*, 1996]. The ratios obtained for the Traill Ø fault are roughly equivalent to those estimated in our study, and their description of the expected behavior fits well with our observations in the step-over region of the Borax Lake fault.

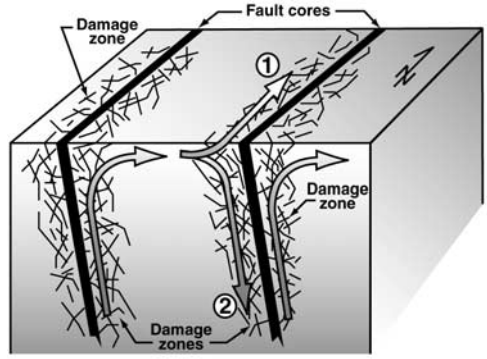


**Figure 3.** Schematic representation of fluid circulation pathways in the Borax Lake fault step-over. Alternate conceptual models of fluid circulation between the fault splays, as discussed in the text, are labeled "1" and "2".

[13] To the best of our knowledge, these are the first published in-situ observations of fluid circulation pathways in an active fault system. Our field observations indicate that the Borax Lake fault acts as a conduit for flow parallel to the fault plane, and as a barrier to fluid flow normal to the plane of the fault, in agreement with the conceptual models of previous investigators [e.g., *Caine et al.*, 1996; *Evans et al.*, 1997; *Jourde et al.*, 2002]. Furthermore, our data imply relatively complex circulation patterns in the area of the fault step-over that include vertical upward discharge of geothermal fluids, lateral migration in the shallow subsurface, and possible structurally-controlled recharge from fluids moving downward along the damage zone of at least one of the two fault splays. Although these types of complex flow circulation patterns are likely to be present in most fault-controlled flow systems, they are generally neglected in conceptual and numerical models. Future studies may help refine our understanding of this important aspect of subsurface fluid flow.

[14] **Acknowledgments.** The authors would like to thank K. N. Nicholson, A. Colter, L. Garringer and K. Link for assistance with data collection. In addition, we would like to thank the two reviewers for their very helpful suggestions. This work received funding from Idaho/EPSCoR and the National Science Foundation (award EPS – 0132626).

## References

Antonellini, M., and A. Aydin (1994), Effect of faulting on fluid flow in porous sandstones: Petrophysical properties, *AAPG Bull.*, *78*, 355–377.

Barton, C. A., M. D. Zoback, and D. Moos (1995), Fluid flow along potentially active faults in crystalline rock, *Geology*, *23*, 683–686.

Blackwell, D. D., S. A. Kelley, and R. C. Edmiston (1986), Analysis and interpretation of thermal data from the Borax Lake geothermal prospect, Oregon, *Trans. Geotherm. Resour. Coun.*, *10*, 169–174.

Bredehoeft, J. D., and I. S. Papadopulos (1965), Rates of vertical groundwater movement estimated from the Earth's thermal profile, *Water Resour. Res.*, *1*, 325–328.

Caine, J. S., J. P. Evans, and C. B. Forster (1996), Fault zone architecture and permeability structure, *Geology*, *24*, 1025–1028.

Carreón-Diazconti, C., S. T. Nelson, A. L. Mayo, D. G. Tingey, and M. Smith (2003), A mixed groundwater system at Midway, UT: Discriminating superimposed local and regional discharge, *J. Hydrol.*, *273*, 119–138.

Cummings, M. L., A. M. St. John, and N. C. Sturchio (1993), Hydrogeochemical characterization of the Alvord Basin geothermal area, Harney County, Oregon, USA, paper presented at 15th New Zealand Geothermal Workshop, Geotherm. Inst., Univ. of Auckland, Auckland, New Zealand.

Curewitz, D., and J. A. Karson (1997), Structural settings of hydrothermal outflow: Fracture permeability maintained by fault propagation and interaction, *J. Volcanol. Geotherm. Res.*, *79*, 149–168.

Evans, J. P., C. B. Forster, and J. V. Goddard (1997), Permeability of fault-related rocks, and implications for hydraulic structure of fault zones, *J. Struct. Geol.*, *19*(11), 1393–1404.

Fairley, J. P., and J. J. Hinds (2004), Permeability distribution in an active Great Basin fault zone, *Geology*, *32*, 825–828.

Fairley, J. P., J. Heffner, and J. J. Hinds (2003), Geostatistical evaluation of permeability in an active fault zone, *Geophys. Res. Lett.*, *30*(18), 1962, doi:10.1029/2003GL018064.

Favara, R., F. Grassa, S. Inguaggiato, and M. Valenza (2001), Hydrogeochemistry and stable isotopes of thermal springs: Earthquake-related chemical changes along Belice Fault (Western Sicily), *Appl. Geochem.*, *16*, 1–17.

Ge, S. (1998), Estimation of groundwater velocity in localized fracture zones from well temperature profiles, *J. Volcanol. Geotherm. Res.*, *84*, 93–101.

Jourde, H., E. A. Flodin, A. Aydin, L. J. Durlofsky, and X. H. Wen (2002), Computing permeability of fault zones in Eolian sandstone from outcrop measurements, *AAPG Bull.*, *86*, 1187–1200.

Kato, A., A. Sakaguchi, S. Yoshida, H. Yamaguchi, and Y. Kaneda (2004), Permeability structure around an ancient exhumed subduction-zone fault, *Geophys. Res. Lett.*, *31*, L06602, doi:10.1029/2003GL019183.

Koski, A. K., and S. A. Wood (2004), The geochemistry of geothermal waters in the Alvord Basin, southeastern Oregon, paper presented at 11th International Symposium on Water-Rock Interaction, Energy and Environ. Dir. of Lawrence Livermore Natl. Lab., Saratoga Springs, New York.

Lu, N., and S. Ge (1996), Effect of horizontal heat and fluid flow on the vertical temperature distribution in a semiconfining layer, *Water Resour. Res.*, *32*, 1449–1453.

Martin, R., K. A. Rodgers, and P. R. L. Browne (2000), Aspects of the distribution and movement of aluminum in the surface of the Te Kopia geothermal field, Taupo Volcanic Zone, New Zealand, *Appl. Geochem.*, *15*, 1121–1136.

Mayo, A. L., et al. (2003), Active and inactive groundwater flow systems: Evidence from a stratified, mountainous terrain, *Geol. Soc. Am. Bull.*, *115*, 1456–1472.

Schneider, T. R., and W. D. McFarland (1995), Hydrologic data and description of a hydrologic monitoring plan for the Borax Lake area, Oregon, *U.S. Geol. Surv. Open File Rep.*, 95–367.

Smith, L., C. Forster, and J. Evans (1990), Interaction of fault zones, fluid flow, and heat transfer at the basin scale, in *Hydrogeology of Low Permeability Environments: From a Special Symposium at the 28th International Geological Congress, Washington, D.C., U.S.A., July 9–19, 1989, Hydrogiology*, vol. 2, edited by S. P. Neuman and I. Neretnieks, pp. 41–67, Verlag Heinz Heise, Hanover, Germany.

Vermilye, J. M., and C. H. Scholz (1998), The process zone: A microstructural view of fault growth, *J. Geophys. Res.*, *103*, 12,223–12,237.

J. P. Fairley and J. J. Hinds, Department of Geological Sciences, University of Idaho, Moscow, ID 83844–3022, USA. (jfairley@uidaho.edu)